Numerical Estimates of Generalized Dimensions $D(q)$ For Negative q

Romualdo Pastor-Satorras*
Departament de Física Fonamental, Facultat de Física, Universitat de Barcelona
Diagonal 647, E-08028 Barcelona (Spain)
Departament de Recerca Científica, Museu de la Ciència de la Fundació "la Caixa"
Teodor Roviralta 55, E-08022 Barcelona (Spain)

Rudolf H. Riedi†
Yale University, Mathematics Department
10 Hillhouse Ave, New Haven CT 06520-8283 (USA)
(July 23, 1995)

Usual box-counting algorithms are unefficient for computing generalized fractal dimensions $D(q)$ in the range of $q < 0$. In this Letter we review the properties of a new algorithm [R. H. Riedi, J. Math. Anal. Appl. **189**, 462 (1995)] specifically devised to deal with large negative q. We discuss the numerical implementation of this algorithm, providing evidence for its better performance. In particular, we throw some light on the structure of the Hénon attractor.

PACS number(s): 05.45.+b, 47.53.+n, 47.10.+g

A great deal of effort has been devoted in the last years to the study of the fractal patterns [1] exhibited by some physical systems such as diffusion-limited aggregates [2], percolation clusters [3], and chaotic attractors of nonlinear dynamical systems [4]. It has become clear, however, that many natural fractal objects are actually *multifractals* [5,6], that is, they are composed of an infinite set of interwoven subfractals, characterized by Hölder exponents α and a *multifractal spectrum* $f(\alpha)$ (see [6,7] and references therein). The usual fixed-size box-counting multifractal formalism for a general measure μ on $\mathbb{R}^d$ considers the so-called *partition sum* $Z_\varepsilon(q) = \sum_{\mu(B)\neq 0}(\mu(B))^q$ where the sum runs over all boxes B of size ε taken from an ε-grid G_ε, i.e.

$$B = \prod_{k=1}^{d} [l_k\varepsilon, (l_k+1)\varepsilon[\,,$$

l_k being integral numbers. The *generalized dimensions* $D(q)$ [8–10] are then defined by

$$D(q) = \frac{1}{q-1}\lim_{\varepsilon\to 0}\frac{\log_{10} Z_\varepsilon(q)}{\log_{10}\varepsilon}. \qquad (1)$$

The function $D(q)$ is non increasing as a consequence of the convexity of $(\cdot)^q$ and of the boundedness of μ, that is, $\sum_B \mu(B) = \text{const} = \varepsilon^0$. The $f(\alpha)$ spectrum is given by the Legendre transformation of $(q-1)D(q)$ [6,7,10].

These definitions, though temptingly simple and rigorous, cause problems even in their pure mathematical application. To be more precise, the limit (1), if it exists, can only be ∞ for $q < 0$ [7,11]. This is due to boxes B with unnaturally small measure overwhelming the function Z. In certain cases the variable ε used in the eq. (1) can be restricted to a sequence ε_n in order to give meaningful results [7,11]. A limit obtained in this way, however, depends strongly on the choice of ε_n and requires, thus, *a priori* knowledge of the multiplicative structure one wants to analyze. Serious problems arise also in any attempt to translate this notion into a numerical algorithm, which we will call *Standard Algorithm* (SA) in the following, and which computes $D(q)$ as the slope of a least-squares fitting of $\log_{10}(Z_\varepsilon(q))/(q-1)$ against $\log_{10}(\varepsilon)$. First, one has to choose a sequence ε_n with the problems just mentioned. In addition, a scaling behavior will only be observed in a restricted *scaling region* of ε since the set of data is finite. SA is slowly convergent and it works well only for $q > 1$ and only for measures in $\mathbb{R}^d$ with $d \leq 2$, being especially problematic the region $q < 0$ [12,13]. Some attempts have been made in order to design efficient fixed-size box-counting algorithms [14–16], but all of them fail when dealing with $q < 0$.

One of us (RR) proposed recently [7,11] a new box-counting approach, the so-called *Enlarged Box Algorithm* (EBA), devised to overcome the drawbacks for negative q. The basic idea is very simple: As we do not assume *a priori* knowledge on the geometrical structure of the distribution μ we cannot prevent that some boxes B will meet μ only in a very small part, say a corner of B. Such a box B is, hence, a very poor approximation of a ball centered in a point on the distribution. Multifractal analysis is bound, on the other hand, to characterize μ by its *local* scaling behavior, meaning that we expect the measure of a ball centered on x being roughly equal to a power of its diameter ε, that is $\mu(U_\varepsilon(x)) \simeq \varepsilon^\alpha$. The Legendre path is legitimate only if the sets B appearing in Z are good approximations of balls $U_\varepsilon(x)$ centered in a point x on μ, since it relies essentially on the argument

$$\begin{aligned} Z_\varepsilon(q) &= \sum_\alpha \sum_{\mu(B)\simeq\varepsilon^\alpha} (\mu(B))^q \\ &\simeq \sum_\alpha (1/\varepsilon)^{f(\alpha)}\varepsilon^{q\alpha} \simeq \varepsilon^{\min\{q\alpha - f(\alpha)\}}, \end{aligned}$$

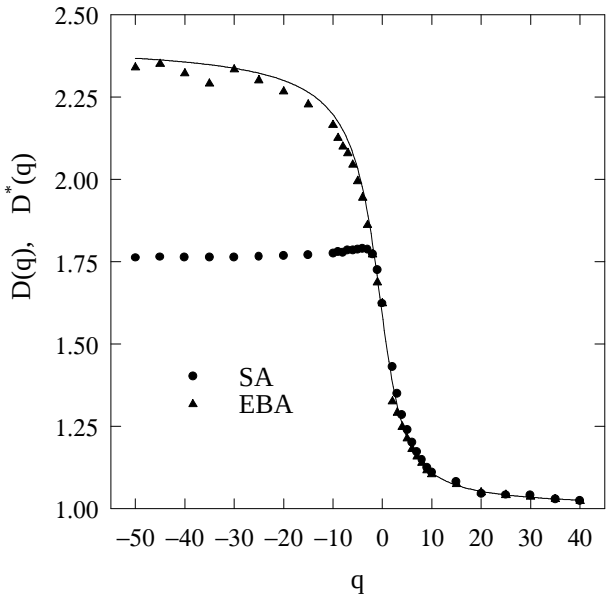

FIG. 1. Generalized dimensions from SA and EBA for the deterministic measure on a Sierpinsky Gasket. Errorbars are about the size of the points, unless in SA, for $q < 0$. The solid line corresponds to the analytical result eq. (6).

(see [6,7,11,17]). For large positive q, mismatching boxes as described above can be neglected since their contribution to Z is almost null. To the contrary for negative q.

From the numerical point of view the best way to cure this problem is to take the measure of *extended boxes* B^*, constructed by expanding a given box B by a factor 3, and defined by

$$B^* = \prod_{k=1}^{d} [(l_k - 1)\varepsilon, (l_k + 1 + 1)\varepsilon[\,,$$

and form a new partition sum Z^* [7]. The new measurement of the sets $B \in G_\varepsilon$, $\mu^*(B) \equiv \mu(B^*)$, is actually not a measure but a capacity (since it is monotonous but not additive). In addition, μ^* is clearly not normalized. It is, however, bounded on each G_ε since B^* is the union of 3^d boxes from G_ε, hence $\sum_{G_\varepsilon} \mu^*(B) \leq 3^d$. The extended partition sum Z^* is defined by

$$Z^*_\varepsilon(q) = \sum_{\mu(B)\neq 0} (\mu^*(B))^q. \qquad (2)$$

The key point in this definition is that the condition of the sum is given by $\mu(B) \neq 0$ and not by $\mu^*(B) \neq 0$ [7]. This condition guarantees that the cubes we consider are indeed good representatives of balls centered in points of the distribution. In particular, Z^*_ε is essentially different from $Z_{3\varepsilon}$. Consequently, we define the *extended generalized dimensions* as

$$D^*(q) = \frac{1}{q-1} \lim_{\varepsilon \to 0} \frac{\log_{10} Z^*_\varepsilon(q)}{\log_{10} \varepsilon} \qquad (3)$$

From a theoretical point of view, $D^*(q)$ performs much better than $D(q)$: It can be proven [7] that the limit (3) is the same if the continuous ε is restricted to a sequence ε_n with $\varepsilon_{n+1} \geq \nu\varepsilon_n$ for some $\nu > 0$. In addition, $D^*(q)$ is invariant under bilipschitz coordinate transformations, it coincides with $D(q)$ (eq. (1)) for $q \geq 0$ and produces the expected, meaningful results for self-similar measures. From a numerical point of view, the implementation of EBA is a more efficient algorithm than SA, as we are about to show.

We applied SA and EBA to distributions given by a sample of N points from the trajectory of some dynamical system. Given an ε-grid of boxes of side ε, the occupation number $n_i(\varepsilon)$ of the i-th box is defined as the number of sample points it contains. The measure μ_i of box B_i is the fraction of time which a generic trajectory on the attractor spends in the i-th box B_i [9], and is roughly equal to $n_i(\varepsilon)/N$. The implementation of SA thus computes $D(q)$ as the slope of a linear fit of

$$\log_{10} Z_\varepsilon(q) = \log_{10} \Big(\sum_i \big(n_i(\varepsilon)\big)^q \Big) \qquad (4)$$

against $\log_{10} \varepsilon$. Note that we have dropped the normalization factor $N = \sum_i n_i(\varepsilon)$ since it is independent of ε.

To implement EBA, we replace the occupation numbers $n_i(\varepsilon)$ by the extended occupation numbers $n^*_i(\varepsilon)$ which are defined by

$$n^*_i(\varepsilon) = \sum_{j:\, B_j \subseteq B^*_i} n_i(\varepsilon),$$

that is, the number of sample points contained in the box B_i and its neighboring boxes. The implementation of EBA, thus, obtains $D^*(q)$ as the slope of a linear fit of

$$\log_{10} Z^*_\varepsilon(q) = \log_{10} \Big(\sum_i \big(n^*_i(\varepsilon)\big)^q \Big) \qquad (5)$$

against $\log_{10} \varepsilon$. As with SA we do not include a normalization with the advantage of good numerical behavior for large $|q|$, the object of our main interest. This procedure might, however, affect the monotony of $D^*(q)$ since $Z^*_\varepsilon(1)$ is not a constant in ε.

In order to check the accuracy of our method, we have applied both SA and EBA to a self-similar deterministic multifractal measure on $\mathbb{R}^2$ constructed with the 'Chaos Game' [18], and generated by iteratively applying the following set of transformations ω_k at random, with probabilities p_k:

$$\begin{aligned} \omega_1(x,y) &= \big(x/2, (y+1)/2\big) & p_1 &= 3/16, \\ \omega_2(x,y) &= \big((x+1)/2, (y+1)/2\big) & p_2 &= 5/16, \\ \omega_3(x,y) &= \big(x/2, y/2\big) & p_3 &= 8/16. \end{aligned}$$

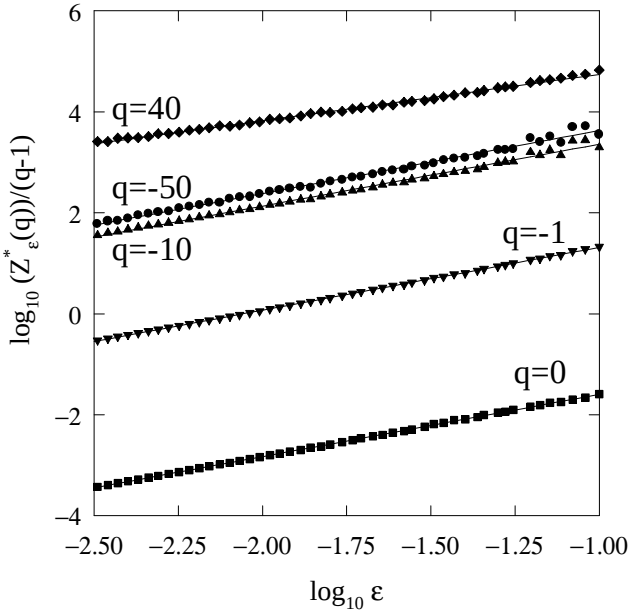

FIG. 2. Log-log plot of the extended partition sum Z^* of the natural measure on the Hénon attractor as a function of ε, for different values of q.

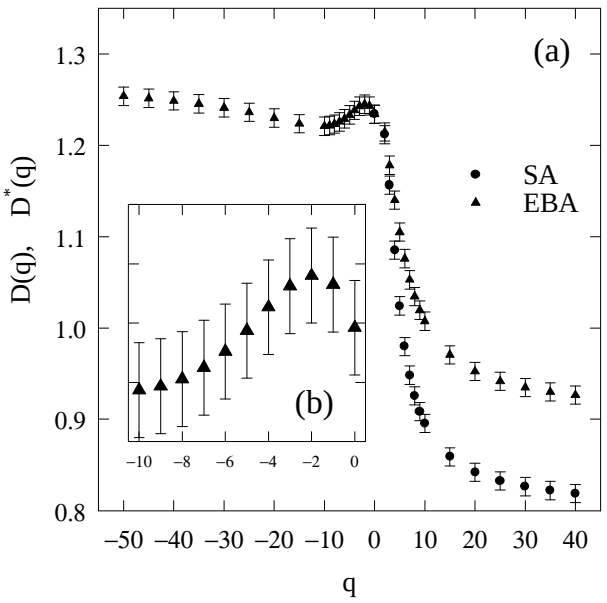

FIG. 3. a) Generalized dimensions from SA and EBA for the natural measure on the Hénon attractor. Being meaningless, the values of SA for $q < 0$ have not been plotted. b) Detail of the region $-10 \leq q \leq 0$.

This allows a comparison of our numerical results with the analytical spectrum D_q given by [7,10]

$$D_q = -\frac{1}{q-1}\log_2\left(p_1^q + p_2^q + p_3^q\right). \qquad (6)$$

We have analyzed 50 different realizations, each one composed by $N = 50,000$ points. Linear regressions were performed over an interval of 1.5 decades.

Fig. 1 depicts the generalized dimensions D and D^* obtianed from SA and EBA, respectively. Statistical errors from the regression algorithms provide error bars of about 0.01 (except for SA at negative q values). Apearently, both SA and EBA provide fairly good results for $q \geq -2$, EBA, however, with far better regression coefficients. For $q < -2$, SA suffers from unacceptable regression coefficients and large error bars. On the other hand, EBA is in excellent agreement with the analytical values over the whole range of q (compare Table I).

We also considered the standard Hénon attractor [19], with parameters $a = 1.4$ and $b = 0.3$. Fig. 2 shows the scaling region of the extended partition sum Z^* for different values of q. The linear fits are excellent even for a negative value as large as $q = -50$. In Fig. 3(a) we have plotted $D(q)$ and $D^*(q)$ computed from 50 different realizations of the attractor, each one composed by $N = 150,000$ points. Table II shows some numerical values, together with theoretical predictions and other numerical estimates from box-counting algorithms. Linear regressions were performed over an interval between $\varepsilon_{min} = 10^{-2.5}$ and $\varepsilon_{max} = 10^{-1}$. Fig. 3(a) shows several remarkable features that deserve some deeper coment:

i) $D^*(q) > D(q)$ for $q > 1$. The values computed with SA are similar to those found by other authors by means of fixed-size [20] and fixed-mass [21] box-counting algorithms, while the results from EBA are somewhat larger, out of the error bars, however in agreement with theoretical predictions (see Table II). It is known that the generalized dimensions of chaotic attractors computed from standard box-counting algorithms significantly underestimates the theoretical predictions, a fact considered a fundamental limitation of this kind of algorithms [20]. Table II shows that EBA is in some cases closest to the theoretical estimates, especially for the extended Kaplan-Yorke relation approach in Ref. [22]. We have to note, however, the disagreement with the prediction $D(\infty) \leq 0.84$ from Ref. [12].

ii) $D^*(q)$ shows a striking inflexion in the region $-10 < q < 0$ (see Fig. 3(b)), which hints towards a failure of the Legendre relation. This inflexion is robust and it does not disappear even when shifting the interval of linear

TABLE I. Comparison of some numerical values from SA and EBA with the analytic result D_q (eq. (6)), for the deterministic measure on a Sierpisky Gasket.

Analytical result	SA	EBA
$D_\infty = 1.0000$	—	—
$D_{40} = 1.0256$	$D(40) = 1.02$	$D^*(40) = 1.02$
$D_0 = 1.5850$	$D(0) = 1.62$	$D^*(0) = 1.62$
$D_{-50} = 2.3677$	—	$D^*(-50) = 2.34$
$D_{-\infty} = 2.4150$	—	—

TABLE II. Henon attractor: Comparison of the performance of SA and EBA with both, theoretical predictions and other numerical estimates.

Theoretical	Numerical	SA	EBA
$D(-\infty) = 1.352$[a]	$D(-\infty) \simeq 1.5$[b]	—	$D^*(-50) = 1.26$
$D(-6) \simeq 1.3$[c]	—	—	$D^*(-6) = 1.23$
$D(0) = 1.276$[d]	$D(0) = 1.259$[e]	$D(0) = 1.23$	$D^*(0) = 1.23$
—	$D(2) = 1.199$[e]	$D(2) = 1.21$	$D^*(2) = 1.21$
$D(6) \simeq 1.05$[c]	—	$D(6) = 0.98$	$D^*(6) = 1.08$
—	$D(40) \simeq 0.8$[f]	$D(40) = 0.82$	$D^*(40) = 0.93$
$D(\infty) \leq 0.84$[g]	$D(\infty) \simeq 0.87$[b]		

[a]Ref. [24].
[b]Ref. [21], estimate from Fig. 2.
[c]Ref. [22], estimate from Fig. 1.
[d]Ref. [22].
[e]Ref. [20].
[f]Ref. [20], estimate from Fig. 2.
[g]Ref. [12].

fit or by changing the number of sample points N or normalizing Z^*_ε. Thus, we view it as a very property of the Hénon attractor, perhaps related to its *lacunarity* [1,20], or more likely, caused by a 'phase transition', meaning that the dense and sparse parts of the attractor, i.e. the turnbacks and the 'straight parts', follow slightly different multiplicative laws due to the bending in the turnbacks. For similar phenomena see [23].

iii) As far as we are aware, we have computed for the first time a fixed-size box-counting estimate of $D(-\infty)$ for the Hénon attractor (~ 1.3). This value is in good agreement with theoretical previsions, in which $D(-\infty)$ is conjectured to be 1.352 [24]. We would like to stress, however, the disaccord with the fixed-mass estimate around 1.5 [21] (see Table II).

In this Letter we have contrasted the performances of the Standard (SA) and a more efficient Enlarged Box (EBA) algorithms for computing generalized dimension. For self-similar measures, EBA renders excellent results in the whole range of values of q, with very small error bars and larger correlation coefficients. In analyzing the Hénon attractor, we find dimensions for $q > 0$ which are in closer agreement with theoretical predictions. We have also estimated the spectrum for $q < 0$, obtaining a good performance and values also in good concordance with theory. An inflexion is also found in the spectrum, which can be interpreted as some kind of 'phase transition'.

We thank Jordi Mach for useful discussions and suggestions. RPS gratefully acknowledges a fellowship from the Museu de la Ciència de la Fundació "la Caixa" (Spain). RHR gratefully acknowledges partial support by a ONR grant.

[1] B. B. Mandelbrot, *The Fractal Geometry of Nature*, (W. H. Freeman and Co., New York, 1982).
[2] T. A. Witten and L. M. Sander, Phys. Rev. Lett. **47**, 1400 (1981); Phys. Rev. B **27**, 5686 (1983).
[3] D. Stauffer, *Introduction to Percolation Theory*, (Taylor & Francis, London, 1985).
[4] H. G. Schuster, *Deterministic Chaos*, (VCH, 1988).
[5] B. B. Mandelbrot, *Fractals and Multifractals: Noise, Turbulence, and Galaxies*, (Springer, New York, 1988).
[6] K. J. Falconer, *The Multifractal Spectrum of Statistically Self-similar Measures*, Report PM-93-01 (University of Bristol, 1993).
[7] R. H. Riedi, J. Math. Anal. Appl. **189**, 462 (1995).
[8] P. Grassberger, Phys. Lett. A **97**, 227 (1983).
[9] H. G. E. Hentschel and I. Procaccia, Physica D **8**, 435 (1983).
[10] T. Halsey, M. Jensen, L. Kadanoff, I. Procaccia, and B. Schraiman, Phys. Rev. A **33**, 1141 (1986).
[11] R. H. Riedi, Ph. D. thesis, ETH Zuerich, 1993.
[12] P. Grassberger, R. Badii, and A. Politi, J. Stat. Phys. **51**, 135 (1988).
[13] H. S. Greenside, A. Wolf, J. Swift, and T. Pignataro, Phys. Rev. A **25**, 3453 (1982).
[14] A. Giorgilli, D. Casati. L. Sironi, and L. Galgani, Phys. Lett. A **115**, 202 (1986).
[15] L. S. Liebovitch and T. Toth, Phys. Lett. A **141**, 386 (1989).
[16] A. Block, W. von Bloh, and H. J. Schellnhuber, Phys. Rev. A **42**, 1869 (1990).
[17] K.-S. Lau, J. Func. Anal. **108**, 427 (1992).
[18] M. Barnsley, *Fractals Everywhere*, (Academic Press, New York, 1988).
[19] M. Hénon, Commun. Math. Phys. **50**, 69 (1976).
[20] A. Arneodo, G. Grasseau, and E. J. Kostelich, Phys. Lett. A **124**, 426 (1987).
[21] R. Badii and G. Broggi, Phys. Lett. A **131**, 339 (1988).
[22] R. Badii and A. Politi, Phys. Rev. A **35**, 1288 (1987).
[23] G. H. Gunaratne and I. Procaccia, Phys. Rev. Lett. **59**, 1377 (1987).
[24] H. Hata, T. Morita, K. Tomita, and H. Mori, Prog. Theor. Phys. **78**, 721 (1987).